JCI The Journal of Clinical Investigation

The LIM-homeodomain transcription factor Lmx1b plays a crucial role in podocytes

Claudia Rohr, … , Corinne Antignac, Ralph Witzgall

J Clin Invest. 2002;109(8):1073-1082. https://doi.org/10.1172/JCI13961.

Article **Genetics**

Patients with nail-patella syndrome often suffer from a nephropathy, which ultimately results in chronic renal failure. The finding that this disease is caused by mutations in the transcription factor LMX1B, which in the kidney is expressed exclusively in podocytes, offers the opportunity for a better understanding of the renal pathogenesis. In our analysis of the nephropathy in nail-patella syndrome, we have made use of the *Lmx1b* knockout mouse. Transmission electron micrographs showed that glomerular development in general and the differentiation of podocytes in particular were severely impaired. The glomerular capillary network was poorly elaborated, fenestrae in the endothelial cells were largely missing, and the glomerular basement membrane was split. In addition podocytes retained a cuboidal shape and did not form foot processes and slit diaphragms. Expression of the α4 chain of collagen IV and of podocin was also severely reduced. Using gel shift assays, we demonstrated that LMX1B bound to two AT-rich sequences in the promoter region of *NPHS2*, the gene encoding podocin. Our results demonstrate that Lmx1b regulates important steps in glomerular development and establish a link between three hereditary kidney diseases: nail-patella syndrome (Lmx1b), steroid-resistant nephrotic syndrome (podocin), and Alport syndrome (collagen IV α4).

The LIM-homeodomain transcription factor Lmx1b plays a crucial role in podocytes

Claudia Rohr,[1] Jürgen Prestel,[1] Laurence Heidet,[2] Hiltraud Hosser,[1] Wilhelm Kriz,[1] Randy L. Johnson,[3] Corinne Antignac,[2] and Ralph Witzgall[1]

[1]Institute for Anatomy and Cell Biology I, University of Heidelberg, Heidelberg, Germany
[2]Institut National de la Santé et de la Recherche Médicale, U423, Hôpital Necker, Paris, France
[3]Department of Biochemistry and Molecular Biology, M.D. Anderson Cancer Center, Houston, Texas, USA

Address correspondence to: Ralph Witzgall, University of Heidelberg, Institute for Anatomy and Cell Biology I, Im Neuenheimer Feld 307, 69120 Heidelberg, Germany.
Phone: 49-(0)6221-548686; Fax: 49-(0)6221-544951; E-mail: ralph.witzgall@urz.uni-heidelberg.de.

Received for publication August 13, 2001, and accepted in revised form March 18, 2002.

Patients with nail-patella syndrome often suffer from a nephropathy, which ultimately results in chronic renal failure. The finding that this disease is caused by mutations in the transcription factor LMX1B, which in the kidney is expressed exclusively in podocytes, offers the opportunity for a better understanding of the renal pathogenesis. In our analysis of the nephropathy in nail-patella syndrome, we have made use of the *Lmx1b* knockout mouse. Transmission electron micrographs showed that glomerular development in general and the differentiation of podocytes in particular were severely impaired. The glomerular capillary network was poorly elaborated, fenestrae in the endothelial cells were largely missing, and the glomerular basement membrane was split. In addition podocytes retained a cuboidal shape and did not form foot processes and slit diaphragms. Expression of the α4 chain of collagen IV and of podocin was also severely reduced. Using gel shift assays, we demonstrated that LMX1B bound to two AT-rich sequences in the promoter region of *NPHS2*, the gene encoding podocin. Our results demonstrate that Lmx1b regulates important steps in glomerular development and establish a link between three hereditary kidney diseases: nail-patella syndrome (Lmx1b), steroid-resistant nephrotic syndrome (podocin), and Alport syndrome (collagen IV α4).

J. Clin. Invest. **109**:1073–1082 (2002). DOI:10.1172/JCI200213961.

Introduction

Nail-patella syndrome (also called hereditary onycho-osteodysplasia) is a relatively rare hereditary disease that is primarily characterized by dysplastic nails and missing or hypoplastic patellae. One-third to one-half of the patients, however, also suffer from hematuria and proteinuria and may ultimately even develop chronic renal failure (1). In some affected kidneys, focal glomerulosclerosis, a thickened glomerular basement membrane (GBM), and protein casts can already be seen by light microscopy. Electron microscopic investigations almost invariably have revealed a GBM, which contains both fibrillar inclusions and electron-lucent areas and thus presents with a moth-eaten appearance (e.g., refs. 2, 3). Although one publication reports the increased deposition of fibrinogen (4) and another finds evidence for the decreased cross-linking of collagen IV (5), the pathogenesis of the glomerular phenotype remains unclear.

In 1998 the first mutations that lead to the development of nail-patella syndrome were reported in the *LMX1B* gene (6–8). The findings in patients are corroborated by the fact that the inactivation of *Lmx1b* in mice also leads to a phenotype strongly resembling nail-patella syndrome (9). The LMX1B protein contains two zinc-binding LIM domains at the NH_2-terminus and a homeodomain in the middle; while the Lin-11, Is1-1, Mec-3 (LIM) domains are felt to represent the interface for the interaction with other proteins, the homeodomain is responsible for the binding to DNA. The mutations described so far lead to the absence or the inactivation of the homeodomain, so that the mutated protein will no longer be able to recognize its target genes. Since a mutant *LMX1B* gene has been described that contains a stop codon in the region coding for the first LIM domain and therefore should result in the synthesis of only a very short peptide (8), a dominant negative mechanism for the development of the syndrome is unlikely. One rather has to assume haploinsufficiency, which, however, contrasts with the finding that in the mouse both alleles of the *Lmx1b* gene have to be inactivated to generate a phenotype (9). We have made use of these *Lmx1b* knockout mice in order to better understand the glomerular phenotype, and we demonstrate a link between nail-patella syndrome, Alport syndrome, and steroid-resistant nephrotic syndrome.

Methods

Knockout animals. The inactivation of the murine *Lmx1b* gene was achieved by replacing exons 3–7 with a selection cassette, thus deleting the region encoding the second LIM domain, the homeodomain, and the

COOH-terminal *trans*-activation domain (9). Heterozygous mice were maintained on a C57BL/6 background. Homozygous mice are born at the expected Mendelian ratio but do not survive beyond postnatal day 1; therefore, on the day of birth offspring were killed by decapitation, and the kidneys were removed and processed as described below.

Electron microscopy. For transmission electron microscopy, kidneys were immersion-fixed overnight in 1× PBS/2% glutaraldehyde and then embedded in Epon. Ninety-nanometer-thick sections were used for transmission electron microscopy. Counterstaining was done with osmium and uranyl acetate.

Morphometry. To determine the glomerular tuft area, kidneys were fixed 4 hours at room temperature in 1× PBS/4% paraformaldehyde and then paraffin-embedded. Four-micrometer-thick sections were prepared and stained with hematoxylin and eosin. Approximately ten glomerular tufts (defined as those profiles that had progressed beyond the S-shaped body stage) were counted randomly on every 24th kidney section, thus keeping the same glomerular from being counted twice. For every kidney, 100 glomerular tufts were analyzed and the mean tuft area calculated.

Immunohistochemistry. For cryosections, kidneys were fixed overnight in 1× PBS/4% paraformaldehyde except when anti–collagen IV antibodies were used (see below). After equilibration in 1× PBS/18% sucrose, the kidneys were frozen in liquid nitrogen and stored at –80°C until further use. Seven- to 10-μm-thick cryosections were blocked in 1× PBS/2% BSA before being stained with a primary antibody for 1 hour at room temperature and then overnight at 4°C. The next morning, sections were washed with PBS and stained for 1 hour with the appropriate secondary antibody. For staining with anti–collagen IV antibodies, the kidneys were immediately frozen in liquid nitrogen and stored at –80°C until further use. Seven- to 10-μm-thick cryosections were fixed with acetone for 10 minutes at –20°C and then air-dried. After denaturing the tissue for 60 minutes with 6 M urea/0.1 M glycine, pH 3.5, the sections were washed three times with 1× PBS and then blocked as described above (10).

For paraffin sections, kidneys were fixed 4 hours at room temperature in 1× PBS/4% paraformaldehyde and then paraffin-embedded. Four-micrometer-thick paraffin sections were deparaffinized and rehydrated before being microwaved five times, for 5 minutes each time, in 10 mM sodium citrate. After the microwave treatment, free aldehyde groups were blocked for 15 minutes with 0.1 M NH_4Cl, endogenous biotin was blocked with an Avidin/biotin blocking kit according to the manufacturer's instructions (Vector Laboratories Inc., Burlingame, California, USA), and endogenous peroxidase was inactivated by incubating for 5 minutes with 3% H_2O_2. Immunohistochemical detection was achieved with the R.T.U. VECTASTAIN Universal Elite ABC Kit (Vector Laboratories Inc.) when employing a nonmurine primary antibody, and with the VECTOR M.O.M. Immunodetection Kit (Vector Laboratories Inc.) when employing a murine primary antibody; in both cases diaminobenzidine (DAB) was used as the substrate.

The following primary antibodies were used: a polyclonal rabbit anti–α3 integrin antibody (diluted 1:3,000; Chemicon International Inc., Hofheim, Germany), a polyclonal rabbit anti-nephrin antibody (diluted 1:1,500) (11), a polyclonal chicken anti-podocalyxin antibody (diluted 1:1,500), the polyclonal rabbit anti-podocin antibody P35 (diluted 1:3,000) (12), a polyclonal rabbit anti-synaptopodin antibody (diluted 1:650) (13), a polyclonal rabbit anti-CD2AP antibody (diluted 1:4,000) (14), a polyclonal rabbit anti-entactin antibody (diluted 1:2,000), a polyclonal rabbit anti-fibronectin antibody (diluted 1:600; Sigma-Aldrich Chemie GmbH, Deisenhofen, Germany), a monoclonal mouse anti-dystroglycan antibody (diluted 1:80; Novocastra Laboratories Ltd., Dossenheim, Germany), a polyclonal rabbit anti–collagen IV α4 antibody (diluted 1:800) (15), and a polyclonal rabbit anti-WT1 antibody (diluted 1:500; Santa Cruz Biotechnology Inc., Heidelberg, Germany). Secondary antibodies were Cy3-conjugated goat anti-rabbit IgG (diluted 1:500; Dianova, Hamburg, Germany), Cy3-conjugated donkey anti-chicken IgY (diluted 1:500; Dianova), and biotinylated goat anti-rabbit IgG (diluted 1:250; Vector Laboratories Inc.).

Nonradioactive in situ hybridization. Fixation and sectioning of the kidneys were carried out as outlined above for cryosections. In situ hybridization was performed essentially as described before (16). The following cDNAs were used: a murine 0.45-kbp $VEGF_{120}$ cDNA, a murine Foxc2 cDNA of about 2 kbp, and a murine 3.2-kbp podocin cDNA.

RNase protection assay. Total RNA from newborn mouse kidneys was isolated using the acid-guanidinium-phenol-chloroform technique, and RNase protection assays were carried out according to standard protocols (17). Antisense RNA was prepared by in vitro transcription from the following fragments: a murine CD2AP fragment (IMAGp998N2210255Q2), a human and a murine podocin fragment, a murine synaptopodin fragment (IMAGp998B059189Q2), a murine VEGF fragment, and an 18S cDNA fragment (Ambion Inc., Austin, Texas, USA). In the case of the 18S cDNA, 50 ng of total RNA from newborn mouse kidneys was used; in all other cases, 20 μg of total RNA was analyzed, and corresponding amounts of tRNA from *Escherichia coli* served as negative control.

Transient and stable transfections. COS-7 cells were transiently transfected according to standard protocols with DEAE-dextran and chloroquine (17). A conditionally immortalized murine podocyte cell line (18) was transiently transfected with Lipofectamine 2000 according to the manufacturer's instructions (Life Technologies GmbH, Karlsruhe, Germany). Three days after the transfection, cell lysates were prepared and assayed for luciferase activity. Stably

transfected HtTA-1 cells (HeLa cells expressing the tetracycline transactivator) (19) were established with a poly-L-ornithine–based protocol (20).

Gel shift assays. Gel shift assays and the preparation of nuclear extracts were performed essentially according to standard protocols (17). The full-length human LMX1B cDNA was subcloned into the bacterial expression vector pET21b (Novagen, Madison, Wisconsin, USA), and the recombinant protein was purified according to the manufacturer's instructions. Coupled in vitro transcription and translation was carried out with the TNT T7 Coupled Reticulocyte Lysate System from Promega GmbH, Mannheim, Germany. The following double-stranded oligonucleotides were used for gel shift assays: one from the first intron of the human *COL4A4* gene ("COL4A4": 5′-GAT CCA TGA AAG TAA TTA TTT TCA-3′ and 5′-GAT CTG AAA ATA ATT ACT TTC ATG-3′), and three from the putative promoter region of the human *NPHS2* gene ("–1087," starting at position 1087 upstream from the start codon: 5′-AGA AAC AAA TTA TTA ACA GAA AGT-3′ and 5′-ACT TTC TGT TAA TAA TTT GTT TCT-3′; "–837," starting at position –837: 5′-TAA GCA TTA ATA AAG ACC CTA AAT AAT AAC AGA G-3′ and 5′-CTC TGT TAT TAT TTA GGG TCT TTA TTA ATG CTT A-3′; and "–287," starting at position –287: 5′-CCT GCC CGG GGC CGG CTC TCC CAC-3′ and 5′-GTG GGA GAG CCG GCC CCG GGC AGG-3′). Radioactively labeled oligonucleotides corresponding to 50,000 cpm were incubated for 30 minutes with the indicated source of LMX1B protein and then run on a 5% polyacrylamide gel at 150 V under constant cooling. When supershifts were performed with nuclear extracts, the anti–myc epitope antibody 9E10 was added at the same time as the nuclear extract, and the mixture was also incubated for 30 minutes.

Results

Morphological characterization of the glomerular phenotype. It could already be noticed by gross inspection that the kidneys from *Lmx1b*$^{-/-}$ mice were smaller than those from *Lmx1b*$^{+/+}$ animals, suggesting that renal development in the homozygous knockout animals was lagging behind. An overview of respective kidney sections pointed in the same direction, since there appeared to be less mature glomeruli on kidneys from *Lmx1b*$^{-/-}$ mice. When the mean glomerular tuft area was determined, it was significantly smaller in *Lmx1b*$^{-/-}$ mice (1,426 μm^2) than in *Lmx1b*$^{+/+}$ mice (1756 μm^2) and *Lmx1b*$^{+/-}$ mice (1782 μm^2) ($P < 0.05$, ANOVA).

Transmission electron microscopy of glomeruli from *Lmx1b*$^{-/-}$ mice clearly showed that the glomeruli were not fully differentiated. In contrast to wild-type kidneys, in which a branched capillary network had developed in the juxtamedullary glomeruli (Figure 1a), the capillaries in the glomeruli from homozygous knockout mice had not branched (Figure 1b). Furthermore, we noticed that the glomerular endothelial cells of the knockout mice were less fenestrated (Figure 1, c and d). In order to gather preliminary evidence for why no branching had taken place

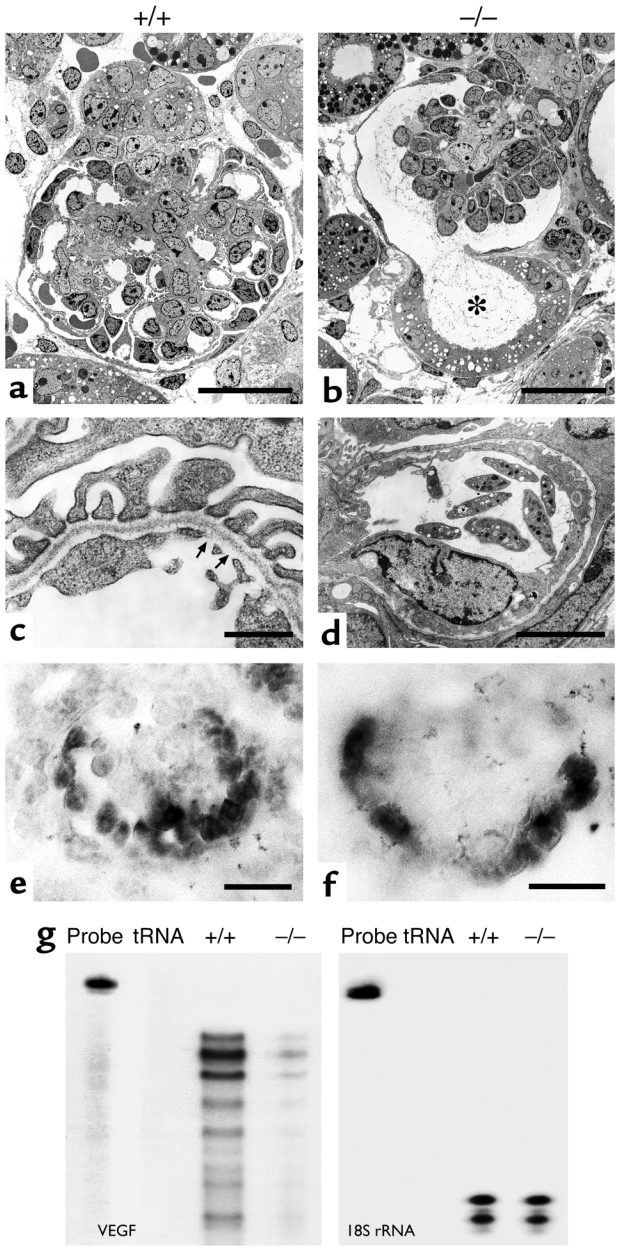

Figure 1
Development of the glomerular capillaries in *Lmx1b*$^{-/-}$ mice. A comparison between newborn wild-type (**a**) and homozygous knockout (**b**) mice demonstrates the severely retarded outgrowth of glomerular capillaries when the *Lmx1b* gene is inactivated. Furthermore, a fibrillar material can be detected in Bowman's space and adjoining proximal tubules of *Lmx1b*$^{-/-}$ mice (asterisk in **b**). At a higher magnification, the reduction and sometimes even complete lack of fenestrae in the endothelium can be seen in the knockout mice (**d**) (arrows in **c** point to fenestrae in the glomerular endothelium of wild-type mice). Although by in situ hybridization VEGF mRNA can be detected in the podocytes of both wild-type (**e**) and *Lmx1b*$^{-/-}$ (**f**) mice, an RNase protection assay with 20 μg of total kidney RNA (prepared from five *Lmx1b*$^{+/+}$ and four *Lmx1b*$^{-/-}$ mice) demonstrates reduced levels of VEGF mRNA in kidneys from the knockout mice (tRNA served as a negative control). A protection assay with a probe directed against 18S rRNA shows that the RNA concentration was determined correctly (**g**). Bar: 20 μm (**a**, **b**, **e**, and **f**), 0.5 μm (**c**), 4 μm (**d**).

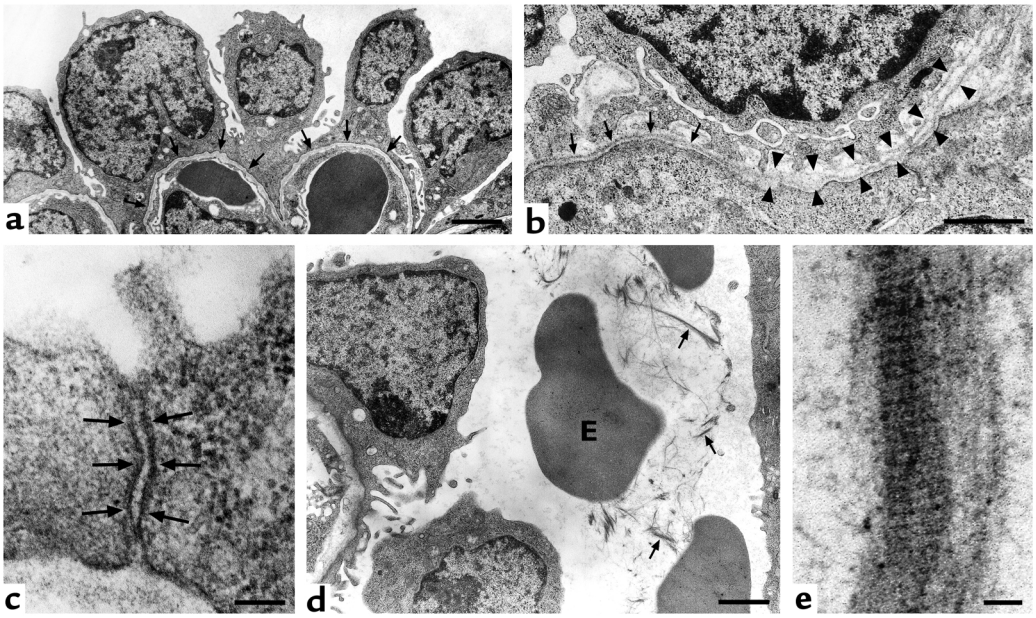

Figure 2
Podocyte differentiation in *Lmx1b*$^{-/-}$ mice. Podocytes in newborn homozygous knockout animals do not spread out over the GBM (arrows) but retain a cuboidal shape (**a**). In many areas the GBM was split (**b** shows a transition between a one-layered GBM marked by arrows and a split GBM marked by arrowheads). In no glomerulus did we notice foot processes and slit diaphragms, but adjacent podocytes were connected by structures resembling adherens junctions (**c**; note the cytoplasmic plaques outlined by arrows on either side of the junction). In some glomeruli we also observed erythrocytes (E) and fibrillar material (arrows) in Bowman's space (**d**), which upon higher magnification showed a striated pattern reminiscent of fibrin (**e**). Bar: 2 μm (**a**), 1 μm (**b** and **d**), 100 nm (**c** and **e**).

and why the endothelium contained less fenestrae, we conducted an in situ hybridization and RNase protection assay for VEGF. Although VEGF mRNA was detected in podocytes from both *Lmx1b*$^{+/+}$ and *Lmx1b*$^{-/-}$ mice by in situ hybridization (Figure 1, e and f), in many (but not all) cases there was less VEGF mRNA in kidneys from the knockout mice by RNase protection assay (Figure 1g).

The podocytes of homozygous knockout mice were still cuboidal and had not flattened out over the GBM (Figure 2a). No foot processes and no slit diaphragms were noticed even in the most advanced glomeruli; neighboring podocytes were rather connected by structures resembling adherens junctions (Figure 2c). In addition, the GBM was split (Figure 2b), and a fibrillar material and even erythrocytes were found in Bowman's space and the lumen of adjoining portions of proximal tubules (Figures 1b and 2d). The fibrillar material was striated with a periodicity of about 17 nm (Figure 2e), indicating that it represents fibrin (21).

In humans, nail-patella syndrome is inherited in an autosomal-dominant fashion, but even after 1 year no morphological abnormalities were found in the glomeruli of heterozygous *Lmx1b* knockout mice (data not shown). Additional experiments will have to be performed to determine whether breeding the mutation onto a different background will yield a phenotype in heterozygous mice.

α3 Integrin, podocalyxin, and nephrin, but not podocin, are expressed by podocytes of Lmx1b$^{-/-}$ *mice.* The lack of foot processes and slit diaphragms prompted us to investigate the expression pattern of podocyte surface proteins, which have been shown to contribute to the establishment of the glomerular filtration barrier. Both the lack of the α3 integrin subunit (22) and the lack of the highly charged protein podocalyxin (23) in mice lead to the absence of foot processes. By immunohistochemistry, however, α3 integrin and podocalyxin could still be easily detected in the podocytes of homozygous knockout mice (Figure 3, a–d). Mutations in *NPHS1*, the gene coding for nephrin, are responsible for congenital nephrotic syndrome of the Finnish type (24). Nephrin has been localized to the slit diaphragm (11, 25, 26), and patients with this disease typically lack a slit diaphragm (27). It was therefore somewhat surprising to find out that nephrin also was still present in the glomeruli of *Lmx1b*$^{-/-}$ mice (Figure 3, e and f).

The result was very different when the expression pattern of podocin, which is mutated in patients with steroid-resistant nephrotic syndrome (28–31), was examined. While podocin protein could be easily detected by immunohistochemistry in the glomeruli of wild-type mice (Figure 4a), it was absent in the glomeruli of *Lmx1b*$^{-/-}$ mice (Figure 4b). This difference could have been caused by an increased instability of the protein due to the absence of foot processes. Therefore we carried out an in situ hybridization with podocin antisense RNA to determine whether podocin mRNA was present in podocytes, but we were unable to find any (Figure 4, c and d). In order to confirm those histochemical findings, an RNase protection assay was

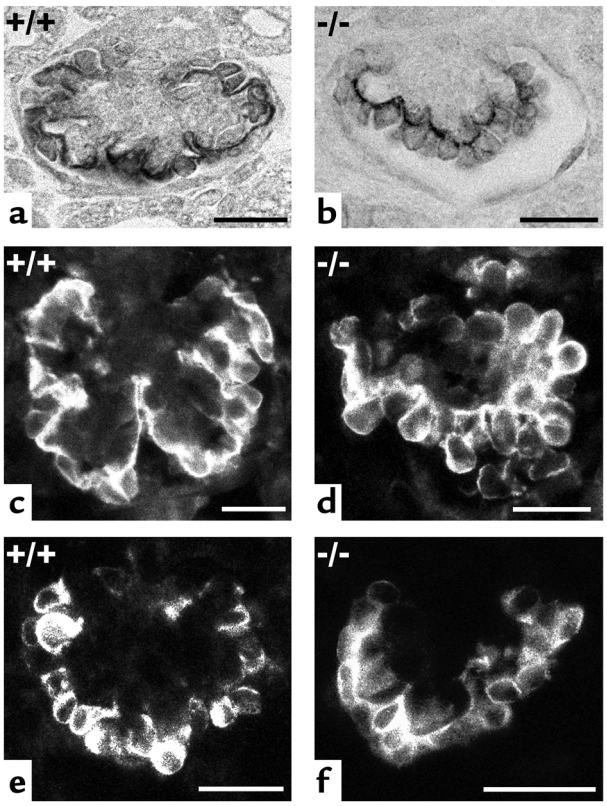

Figure 3
Expression of α3 integrin, podocalyxin, and nephrin in newborn *Lmx1b*$^{-/-}$ mice. By immunohistochemistry, α3 integrin (**a** and **b**), podocalyxin (**c** and **d**), and nephrin (**e** and **f**) were all detected in the glomeruli of wild-type (**a**, **c**, and **e**) and homozygous knockout mice (**b**, **d**, and **f**). Immunohistochemical detection of the proteins in **a** and **b** was done with DAB, in **c**–**f** by fluorescence. Bar: 20 μm (**a**–**f**).

performed with RNA isolated from newborn mouse kidneys. Again, no podocin mRNA was detected in kidneys of *Lmx1b*$^{-/-}$ mice (Figure 4e).

Since the absence of podocin mRNA pointed to a transcriptional defect, the putative promoter region of human *NPHS2*, the gene encoding podocin, was screened for possible LMX1B binding sites. The hamster Lmx1a protein, whose homeodomain is identical to that of human LMX1B (32), recognizes two related AT-rich motifs called the FLAT-E (5′-TAATTA-3′) and FLAT-F (5′-TTAATAAT-3′) elements (33), and it was therefore reasonable to assume that LMX1B binds to similar motifs. We found one perfect FLAT-F element extending from nucleotides 1079 to 1072 and two closely spaced imperfect FLAT-E elements extending from nucleotides 832 to 809 upstream of the start codon in the *NPHS2* promoter. Oligonucleotides containing these elements, but not a GC-rich oligonucleotide closer to the start codon, were recognized from bacterially expressed full-length LMX1B protein in a gel shift assay (Figure 5a). The binding was specific, since the shifts disappeared by competing with an excess of the same unlabeled oligonucleotide but not with an excess of the unlabeled nonspecific oligonucleotide (Figure 5b). Furthermore, the "COL4A4," "–1087," and "–837" oligonucleotides were able to compete with one another (data not shown). To rule out the possibility that the bacterially expressed protein was not folded correctly, we also employed the in vitro–translated homeodomain of LMX1B and nuclear extracts from stably transfected HeLa cells in gel shift assays. (We used the homeodomain because a nonspecific shift tended to mask the shift obtained with the in vitro–translated full-length LMX1B protein.) Again we demonstrated binding (Figure 5, c and d). To determine whether the recognition of these binding sites by LMX1B in the putative *NPHS2* promoter is sufficient to lead to its activation, we transiently transfected COS-7 cells and a conditionally immortalized murine podocyte cell line (18) with an LMX1B expression plasmid and a luciferase reporter plasmid containing about 4.4 kbp of the putative *NPHS2* promoter region (extending from 4,303 bp

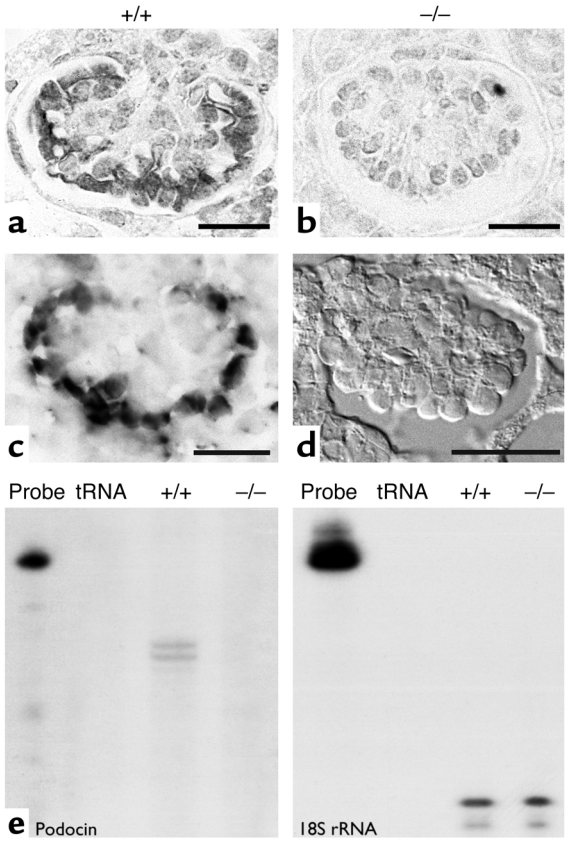

Figure 4
Expression of podocin in newborn *Lmx1b*$^{-/-}$ mice. Podocin protein (**a**) and mRNA (**c**) were present only in podocytes of wild-type mice, not in those of homozygous knockout mice (**b** and **d**). The specificity of these results was corroborated by an RNase protection assay with podocin antisense RNA, where protected bands were observed only with RNA isolated from kidneys of wild-type mice (tRNA served as a negative control). A protection assay with a probe directed against 18S rRNA shows that the RNA concentration was determined correctly (**e**). Immunohistochemical detection of the proteins was done with DAB, and mRNA was detected by nonradioactive in situ hybridization (in order to demonstrate the negative glomerulus, the picture shown in **d** was taken using Nomarski optics). Bar: 20 μm (**a** and **b**), 40 μm (**c** and **d**).

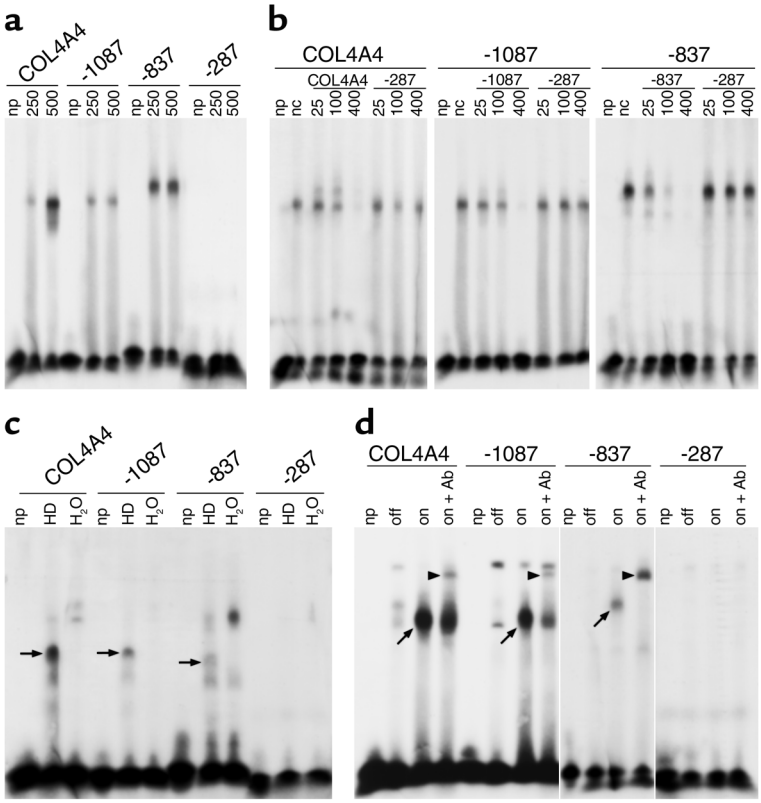

Figure 5
Gel shift assays to demonstrate binding of LMX1B to FLAT-E and FLAT-F elements in the *NPHS2* promoter region. The gel shift assays were carried out with an oligonucleotide from the first intron of the human *COL4A4* gene COL4A4, whose recognition by LMX1B had been demonstrated before (38) and that therefore served as a positive control; an oligonucleotide containing a perfect FLAT-F element (–1087); an oligonucleotide containing two imperfect FLAT-E elements (–837); and a GC-rich oligonucleotide containing neither a FLAT-E nor a FLAT-F element (–287). (**a**) Two hundred fifty and 500 ng of bacterially expressed full-length LMX1B protein recognize not only the binding site in the *COL4A4* intron, but also the perfect FLAT-F and imperfect FLAT-E elements, while the GC-rich oligonucleotide is not bound. np, oligonucleotide with no protein added. (**b**) Competition assays using 500 ng of bacterially expressed full-length LMX1B protein and a 25-fold, 100-fold, and 400-fold molar excess of the indicated unlabeled oligonucleotides demonstrate the specificity of the gel shift. Labeled oligonucleotides are indicated on the top, unlabeled oligonucleotides below. nc, no competing unlabeled oligonucleotide added. (**c**) Four microliters of the in vitro–translated LMX1B homeodomain were incubated with the oligonucleotides described above. It can be easily seen that the homeodomain (HD) recognizes the binding site in the *COL4A4* intron, the perfect FLAT-F element, and the imperfect FLAT-E elements, but not the GC-rich oligonucleotide. Specific bands are indicated by arrows; the other bands can also be seen where no DNA was added to the in vitro transcription/translation reaction (H_2O). (**d**) Nuclear extracts were prepared from stably transfected HeLa cells inducibly expressing a myc epitope–tagged full-length LMX1B protein, and 6 μg of nuclear proteins from noninduced ("off") and induced ("on") cells were used for a gel shift assay. Upon the induction of LMX1B, a clear shift can be recognized with the binding site in the *COL4A4* intron and the perfect FLAT-F and imperfect FLAT-E elements (arrows). The specificity of the shift can be appreciated from the supershifted band appearing upon the addition of the anti–myc epitope antibody 9E10 (arrowhead in "on + Ab" lane).

upstream to 129 bp downstream of the start codon). Even after repeated attempts, however, we could not see a regulatory effect of LMX1B on the reporter plasmid. In addition, we used the stably transfected HeLa cells, which upon the removal of doxycycline inducibly express LMX1B, to determine whether the endogenous podocin gene responded to the induction of LMX1B, but once again no effect was noticed (data not shown).

Expression pattern of actin cytoskeleton–associated and basement membrane proteins in the glomeruli of Lmx1b$^{-/-}$ knockout mice. The absence of podocyte foot processes in the homozygous *Lmx1b* knockout mice could have also been due to a defect in the cytoskeletal apparatus of the podocytes, and we therefore investigated the expression pattern of proteins associated with the actin cytoskeleton, i.e., synaptopodin and CD2AP. Synaptopodin is a proline-rich protein that has been localized to podocyte foot processes and to actin stress fibers (13). The inactivation of the gene encoding CD2AP leads to foot process effacement, and CD2AP also has been shown to interact with nephrin (34, 35). Both proteins, however, were present in the glomeruli of homozygous knockout mice (Figure 6, a–d), although it appeared as if the signal was weaker on those kidney sections. An RNase protection assay demonstrated that roughly equal amounts of CD2AP (Figure 6e), but decreased levels of synaptopodin (Figure 6f), were present in the kidneys of *Lmx1b*$^{-/-}$ mice.

The morphological alterations in the GBM observed in patients with nail-patella syndrome and in the *Lmx1b*$^{-/-}$ mice suggested that important ECM components were lacking. Both nidogen/entactin (Figure 6, g and h) and fibronectin (Figure 6, i and j), however, were present in the GBMs of homozygous knockout mice. We next examined dystroglycan, which has been speculated to be important for the proper arrangement of basement membrane components (36), and again we found no difference between wild-type and homozygous knockout mice (Figure 6, k and l). Another important component of the GBM is represented by collagen IV. While the prospective GBM contains the α1 and α2 chains of collagen IV, an additional network consisting of the α3, α4, and α5 chains is added by the podocyte subsequently (15). Mutations in the latter collagen chains are responsible for Alport syndrome, a hereditary kidney disease eventually leading to chronic renal failure (for review see ref. 37). When the expression of the collagen IV α4 chain was examined in the kidneys of the *Lmx1b*$^{-/-}$ mice, a pronounced downregulation of this subunit was observed (data not shown), as is described in a publication that appeared while this manuscript was in preparation (38).

Expression pattern of podocyte-specific transcription factors. Since it was obvious from the morphological characterization and the lack of podocin and the collagen IV α4 chain that the developmental defect in *Lmx1b*$^{-/-}$ mice affected the podocyte lineage, we tried to determine whether these defects were only due to the lack of Lmx1b, or whether other transcription factors also played a role. The C_2H_2 zinc finger protein WT1 can already be detected in the condensing metanephrogenic mesenchyme, but later the expression of WT1 is restricted to podocytes (39). No difference, however, was observed between the kidneys of wild-type and homozygous knockout mice (Figure 7, a and b).

The inactivation of the *Lmx1b* gene also leads to defects in eye development. In the presence of Lmx1b, two transcription factors of the winged helix family, Foxc1 (also called Mf1, FREAC3, and FKHL7) and Foxc2 (also called Mfh1), are not found in the differentiating corneal stroma, while in the absence of Lmx1b both proteins can be detected in this structure (40). The Foxc2 mRNA had been localized to podocytes before (41), and so we determined its expression pattern in the *Lmx1b* knockout mice. In contrast to the situation in the eye, no obvious differences for Foxc2 were observed in the kidneys of *Lmx1b*$^{-/-}$ and wild-type mice (Figure 7, c and d).

Discussion

The combination of the ultrastructural with the histochemical characterization of the glomeruli from *Lmx1b*$^{-/-}$ mice provides valuable information on the consequences of the inactivation of *Lmx1b* in the kidney. It is obvious that the formation of a fully branched glomerular capillary network depends on intact podocytes. Without fully differentiated podocytes, capillaries will invade the glomerulus, but

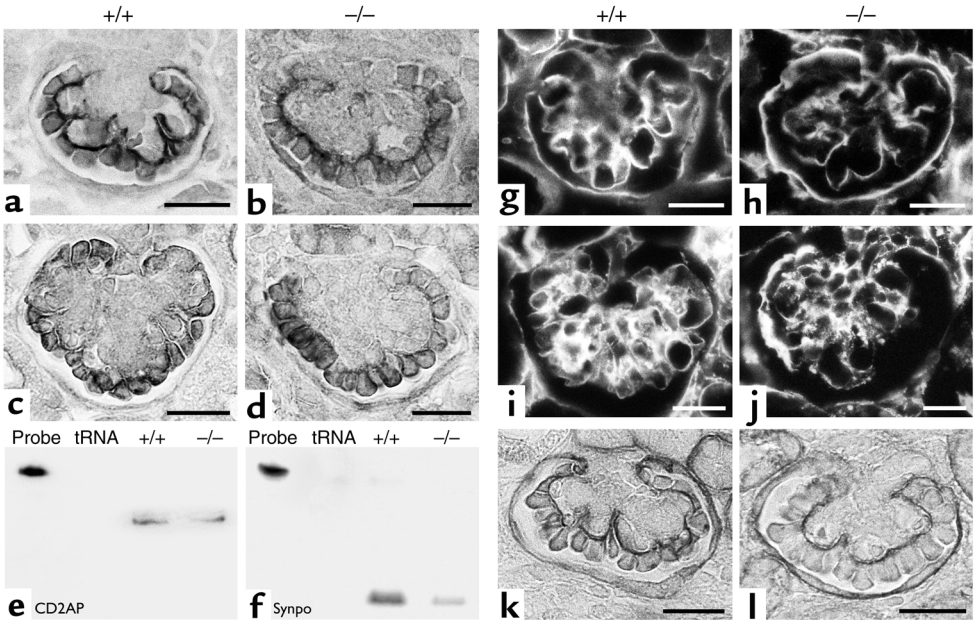

Figure 6

Expression of actin cytoskeleton–associated proteins and GBM components in newborn *Lmx1b*$^{-/-}$ mice. The actin cytoskeleton–associated proteins synaptopodin (**a** and **b**) and CD2AP (**c** and **d**) are both expressed in kidneys of wild-type and homozygous knockout mice. An RNase protection assay with 20 μg of total kidney RNA demonstrates approximately equal levels of CD2AP mRNA (**e**) but reduced amounts of synaptopodin (Synpo) mRNA (**f**) in the knockout mice (tRNA served as a negative control). The protection assay with a probe directed against 18S rRNA is shown in Figure 1. The GBM components nidogen/entactin (**g** and **h**), fibronectin (**i** and **j**), and dystroglycan (**k** and **l**) can all be detected in kidneys of wild-type and homozygous knockout mice. Immunohistochemical detection of the proteins was done with DAB (**a**–**d**, **k** and **l**) and by fluorescence (**g**–**j**). Bars: 20 μm.

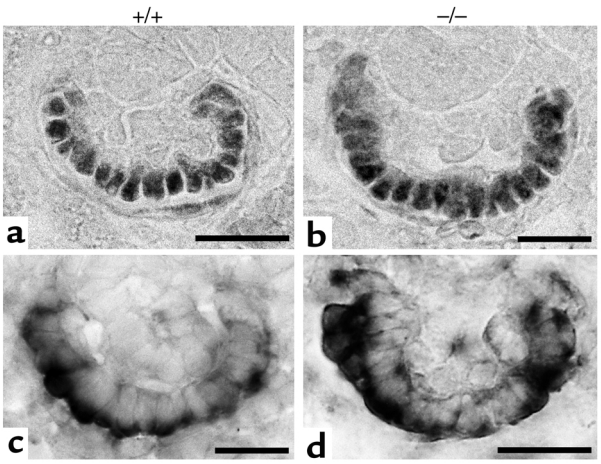

Figure 7
Expression of transcription factors in newborn *Lmx1b*$^{-/-}$ mice. WT1 (**a** and **b**) and Foxc2 (**c** and **d**) are both expressed in kidneys of wild-type and homozygous knockout mice. WT1 protein was detected immunohistochemically with DAB, the Foxc2 mRNA with nonradioactive in situ hybridization. Bar: 20 μm.

they will not branch. It is not completely understood which signals regulate the formation of the glomerular tuft, but previous results from animal studies (42–44) and organ culture experiments (45) argue that VEGF plays an important role in this process. Furthermore, VEGF also seems to regulate the fenestration of endothelial cells (46, 47). Both the retarded branching of the glomerular capillaries and the decreased number of fenestrae in the glomerular endothelium suggest that Lmx1b-deficient podocytes produce less VEGF, and indeed the quantitation of VEGF mRNA by RNase protection assay indicates that podocytes in *Lmx1b*$^{-/-}$ mice secrete less VEGF than do their wild-type counterparts. In this context we wish to point out that the inactivation of a single *VEGF* allele already leads to embryonic lethality (48, 49), which demonstrates the critical dosage effect of VEGF, so that even a subtle decrease in VEGF levels may result in a developmental defect of the glomerular tuft. Alternatively, other pathways like the one based on the interaction between Notch2 and Jag1 (50) may be affected by the absence of Lmx1b.

Podocytes lacking Lmx1b are of a columnar shape and do not form foot processes. To our knowledge, the α3 integrin (22), podocalyxin (23), and Pod1 (51) knockout animals are the only other mice in which podocytic foot processes are lacking *a priori*, whereas in the case of the laminin β2 (52) and CD2AP (34) knockout mice, foot processes form first and process effacement takes place later. It is also noteworthy that the podocytes in the homozygous *Lmx1b* knockout animals are not connected by slit diaphragms. Formation of foot processes may therefore be essential to establish slit diaphragms, although it clearly is not sufficient, since foot processes, but no slit diaphragms, are formed in the absence of nephrin (53). The presence of nephrin in the podocytes of *Lmx1b* knockout mice also argues that nephrin does not suffice to initiate the formation of a slit diaphragm. So far it is a complete mystery how the interdigitating arrangement of foot processes arises and, once established, how it is regulated. Obviously α3 integrin and podocalyxin are critical components in foot process formation, but these proteins are still present in the *Lmx1b*$^{-/-}$ mice. By immunohistochemistry there seemed to be a decreased expression of CD2AP and synaptopodin in the podocytes of Lmx1b-deficient mice, but by RNase protection assay we convincingly found only reduced levels of synaptopodin mRNA in those kidneys. Whether CD2AP is downregulated remains an open question, since total kidney RNA was used in our experiments and CD2AP is also expressed outside the glomerulus in tubules (54), so that a reduction in the glomerulus may go unnoticed in an RNase protection assay. Synaptopodin is an actin-associated protein in the foot processes of podocytes, and therefore its downregulation in the *Lmx1b* knockout mice is not unexpected. Since synaptopodin knockout mice show no structural abnormalities in the glomerulus (55), the reduced expression of synaptopodin in the *Lmx1b* knockout mice very likely is a secondary effect and cannot explain the absence of foot processes.

Another strong candidate to regulate the formation of interdigitating foot processes is podocin. Podocin is mutated in at least a subset of patients with an onset of steroid-resistant nephrotic syndrome in early childhood (28–31). Because proteinuria typically is associated with the absence of foot processes, it is reasonable to assume that foot processes are missing in the podocytes of those patients as well. If it could be determined whether foot processes were never present or whether they disappeared after having formed, the function of podocin would be clearer. Since, in the kidney, both Lmx1b and podocin are exclusively expressed in podocytes and the inactivation of *Lmx1b* results in the absence of podocin, *Nphs2*, the gene coding for podocin, appears as an obvious target for Lmx1b. Indeed, we were able to demonstrate binding of LMX1B to two AT-rich regions in the putative human *NPHS2* promoter region. However, we did not see a regulatory effect of LMX1B on an approximately 4.4-kbp *NPHS2* promoter fragment employing transient transfections in COS-7 cells and in conditionally immortalized podocytes, nor was the endogenous *NPHS2* gene activated in stably transfected HeLa cells. This may indicate that appropriate cofactors are missing in the cell lines used in our experiments. Lmx1b is expressed in a number of other tissues, such as the eye, the brain, and the limb bud, in which no podocin is found, and therefore it may very well be that additional transcription factors play a role in the expression of podocin in the kidney.

The GBM represents another important component of the filtration barrier. While nidogen/entactin, fibronectin, and dystroglycan were present in the GBMs of *Lmx1b*$^{-/-}$ mice, the α4 chain of collagen IV was missing. During the preparation of this

manuscript, the diminished expression of the collagen IV α3 and α4 chains was described in the GBM of *Lmx1b*$^{-/-}$ mice (38). The absence of an α3α4α5 network of collagen IV can explain the split GBM found in the homozygous *Lmx1b* knockout mice and the moth-eaten appearance of the GBM in patients with nail-patella syndrome. It is noteworthy that the genesis of collagen fibrils also is disturbed in the corneal stroma of the *Lmx1b* knockout mice (40).

The severe defects in the podocyte suggest that, in a genetic sense, Lmx1b is located far upstream in the podocyte. WT1, another transcription factor mutated in certain hereditary podocyte diseases (56–58), was present in the podocytes of wild-type and knockout mice, arguing that Lmx1b lies downstream of WT1. We were particularly interested to determine the expression pattern of Foxc2 (also called Mfh1) because of its importance for renal development and previous findings in the eyes of *Lmx1b* knockout mice. Inactivation of the *Foxc2* gene results in only a mild kidney phenotype (59, 60), but compound heterozygotes, in which one allele of the related gene *Foxc1* is inactivated as well, have pronounced renal defects (60). Furthermore, Foxc1 and Foxc2 are not expressed in the differentiating corneal stroma of the normal mouse but are present in that of the *Lmx1b*$^{-/-}$ mouse (40, 61). No differences, however, were seen in the podocytes of homozygous *Lmx1b* knockout mice, for which we offer the following explanation. The human LMX1B protein has been demonstrated to act as a transcriptional activator (62); therefore the *Foxc2* gene is unlikely to be a direct target of Lmx1b during eye development, since it is upregulated and not downregulated in the absence of Lmx1b. Probably Lmx1b acts through at least one intermediary protein, which represses the *Foxc2* gene in the differentiating cornea. This so-far hypothetical intermediary repressor protein may be absent in the podocytes, so that the renal expression of Foxc2 is not affected.

The *Lmx1b* knockout mouse presents an extremely valuable tool to study the differentiation of the podocyte. It apparently mimics the human syndrome, although it is puzzling that nail-patella syndrome is inherited in a dominant fashion in patients, but only the homozygous *Lmx1b* knockout mice show a renal phenotype. Furthermore, LMX1B presents a link between nail-patella syndrome, Alport syndrome, and steroid-resistant nephrotic syndrome, since it regulates the expression of collagen IV α4 and podocin.

Acknowledgments

Antibodies were the generous gifts of Albert Chung (entactin), Larry Holzman (nephrin), David Kershaw (podocalyxin), Jeff Miner (collagen IV α4), Peter Mundel (synaptopodin), and Andrey Shaw (CD2AP), and cDNAs were kindly provided by Georg Breier ($VEGF_{120}$), Brigid Hogan (Foxc2), and Brendan Lee (LMX1B). HtTA-1 cells were a kind gift from Hermann Bujard. Murine CD2AP and synaptopodin cDNAs were purchased from the Deutsches Ressourcenzentrum für Genomforschung GmbH (Ressourcenzentrum und Primärdatenbank) (63). We also acknowledge financial support from the German Research Council (Deutsche Forschungsgemeinschaft, Forschergruppe 406, Mechanismen der Progression des chronischen Nierenversagens) and are grateful for the superb arrangement of the figures by Rolf Nonnenmacher.

1. Bennett, W.M., et al. 1973. The nephropathy of the nail-patella syndrome. Clinicopathologic analysis of 11 kindred. *Am. J. Med.* **54**:304–319.
2. del Pozo, E., and Lapp, H. 1970. Ultrastructure of the kidney in the nephropathy of the nail-patella syndrome. *Am. J. Clin. Pathol.* **54**:845–851.
3. Ben-Bassat, M., Cohen, L., and Rosenfeld, J. 1971. The glomerular basement membrane in the nail-patella syndrome. *Arch. Pathol.* **92**:350–355.
4. Drut, R.M., Chandra, S., Latorraca, R., and Gilbert-Barness, E. 1992. Nail-patella syndrome in a spontaneously aborted 18-week fetus: ultrastructural and immunofluorescent study of the kidneys. *Am. J. Med. Genet.* **43**:693–696.
5. Lubec, B., Arbeiter, K., Ulrich, W., and Frauscher, G. 1995. Hereditary osteo-onycho-renal dysplasia with excess urinary pyridinoline cross-links and abnormal kidney collagen cross-linking. *Nephron*. **70**:255–259.
6. Dreyer, S.D., et al. 1998. Mutations in *LMX1B* cause abnormal skeletal patterning and renal dysplasia in nail patella syndrome. *Nat. Genet.* **19**:47–50.
7. McIntosh, I., et al. 1998. Mutation analysis of *LMX1B* gene in nail-patella syndrome patients. *Am. J. Hum. Genet.* **63**:1651–1658.
8. Vollrath, D., et al. 1998. Loss-of-function mutations in the LIM-homeodomain gene, *LMX1B*, in nail-patella syndrome. *Hum. Mol. Genet.* **7**:1091–1098.
9. Chen, H., et al. 1998. Limb and kidney defects in *Lmx1b* mutant mice suggest an involvement of *LMX1B* in human nail patella syndrome. *Nat. Genet.* **19**:51–55.
10. Heidet, L., Cai, Y., Guicharnaud, L., Antignac, C., and Gubler, M.-C. 2000. Glomerular expression of type IV collagen chains in normal and X-linked Alport syndrome kidneys. *Am. J. Pathol.* **156**:1901–1910.
11. Holzman, L.B., et al. 1999. Nephrin localizes to the slit pore of the glomerular epithelial cell. *Kidney Int.* **56**:1481–1491.
12. Roselli, S., et al. 2002. Podocin localizes in the kidney to the slit diaphragm area. *Am. J. Pathol.* **160**:131–139.
13. Mundel, P., et al. 1997. Synaptopodin: an actin-associated protein in telencephalic dendrites and renal podocytes. *J. Cell Biol.* **139**:193–204.
14. Dustin, M.L., et al. 1998. A novel adaptor protein orchestrates receptor patterning and cytoskeletal polarity in T-cell contacts. *Cell.* **94**:667–677.
15. Miner, J.H., and Sanes, J.R. 1994. Collagen IV α3, α4, and α5 chains in rodent basal laminae: sequence, distribution, association with laminins, and developmental switches. *J. Cell Biol.* **127**:879–891.
16. Obermüller, N., Gretz, N., Kriz, W., Reilly, R.F., and Witzgall, R. 1998. The swelling-activated chloride channel ClC-2, the chloride channel ClC-3, and ClC-5, a chloride channel mutated in kidney stone disease, are expressed in distinct subpopulations of renal epithelial cells. *J. Clin. Invest.* **101**:635–642.
17. Ausubel, F.A., et al. 1996. *Current protocols in molecular biology.* John Wiley & Sons. New York, New York, USA.
18. Mundel, P., et al. 1997. Rearrangements of the cytoskeleton and cell contacts induce process formation during differentiation of conditionally immortalized mouse podocyte cell lines. *Exp. Cell Res.* **236**:248–258.
19. Gossen, M., and Bujard, H. 1992. Tight control of gene expression in mammalian cells by tetracycline-responsive promoters. *Proc. Natl. Acad. Sci. USA.* **89**:5547–5551.
20. Dong, Y., Skoultchi, A.I., and Pollard, J.W. 1993. Efficient DNA transfection of quiescent mammalian cells using poly-L-ornithine. *Nucleic Acids Res.* **21**:771–772.
21. Margaretten, W., Csavossy, I., and McKay, D.G. 1967. An electron microscopic study of thrombin-induced disseminated intravascular coagulation. *Blood*. **29**:169–181.
22. Kreidberg, J.A., et al. 1996. Alpha 3 beta 1 integrin has a crucial role in kidney and lung organogenesis. *Development*. **122**:3537–3547.
23. Doyonnas, R., et al. 2001. Anuria, omphalocele, and perinatal lethality in mice lacking the CD34-related protein podocalyxin. *J. Exp. Med.* **194**:13–27.
24. Kestilä, M., et al. 1998. Positionally cloned gene for a novel glomerular protein — nephrin — is mutated in congenital nephrotic syndrome. *Mol. Cell.* **1**:575–582.
25. Holthöfer, H., et al. 1999. Nephrin localizes at the podocyte filtration slit area and is characteristically spliced in the human kidney. *Am. J. Pathol.* **155**:1681–1687.
26. Ruotsalainen, V., et al. 1999. Nephrin is specifically located at the slit diaphragm of glomerular podocytes. *Proc. Natl. Acad. Sci. USA.* **96**:7962–7967.

27. Patrakka, J., et al. 2000. Congenital nephrotic syndrome (NPHS1): features resulting from different mutations in Finnish patients. *Kidney Int.* **58**:972–980.
28. Boute, N., et al. 2000. *NPHS2*, encoding the glomerular protein podocin, is mutated in autosomal recessive steroid-resistant nephrotic syndrome. *Nat. Genet.* **24**:349–354.
29. Caridi, G., et al. 2001. Prevalence, genetics, and clinical features of patients carrying podocin mutations in steroid-resistant nonfamilial focal segmental glomerulosclerosis. *J. Am. Soc. Nephrol.* **12**:2742–2746.
30. Frishberg, Y., et al. 2002. Mutations in *NPHS2* encoding podocin are a prevalent cause of steroid-resistant nephrotic syndrome among Israeli-Arab children. *J. Am. Soc. Nephrol.* **13**:400–405.
31. Karle, S.M., et al. 2002. Novel mutations in *NPHS2* detected in both familial and sporadic steroid-resistant nephrotic syndrome. *J. Am. Soc. Nephrol.* **13**:388–393.
32. Iannotti, C.A., et al. 1997. Identification of a human LMX1 (LMX1.1)-related gene, LMX1.2: tissue-specific expression and linkage mapping on chromosome 9. *Genomics*. **46**:520–524.
33. German, M.S., Wang, J., Chadwick, R.B., and Rutter, W.J. 1992. Synergistic activation of the insulin gene by a LIM-homeodomain protein and a basic helix-loop-helix protein: building a functional insulin minienhancer complex. *Genes Dev.* **6**:2165–2176.
34. Shih, N.-Y., et al. 1999. Congenital nephrotic syndrome in mice lacking CD2-associated protein. *Science*. **286**:312–315.
35. Shih, N.-Y., et al. 2001. CD2AP localizes to the slit diaphragm and binds to nephrin via a novel C-terminal domain. *Am. J. Pathol.* **159**:2303–2308.
36. Regele, H.M., et al. 2000. Glomerular expression of dystroglycans is reduced in minimal change nephrosis but not in focal segmental glomerulosclerosis. *J. Am. Soc. Nephrol.* **11**:403–412.
37. Kashtan, C.E. 1998. Alport syndrome and thin glomerular basement membrane disease. *J. Am. Soc. Nephrol.* **9**:1736–1750.
38. Morello, R., et al. 2001. Regulation of glomerular basement membrane collagen expression by *LMX1B* contributes to renal disease in nail patella syndrome. *Nat. Genet.* **27**:205–208.
39. Pritchard-Jones, K., et al. 1990. The candidate Wilms' tumour gene is involved in genitourinary development. *Nature*. **346**:194–197.
40. Pressman, C.L., Chen, H., and Johnson, R.L. 2000. *Lmx1b*, a LIM homeodomain class transcription factor, is necessary for normal development of multiple tissues in the anterior segment of the murine eye. *Genesis*. **26**:15–25.
41. Miura, N., Wanaka, A., Tohyama, M., and Tanaka, K. 1993. MFH-1, a new member of the fork head domain family, is expressed in developing mesenchyme. *FEBS Lett.* **326**:171–176.
42. Kitamoto, Y., Tokunaga, H., and Tomita, K. 1997. Vascular endothelial growth factor is an essential molecule for mouse kidney development: glomerulogenesis and nephrogenesis. *J. Clin. Invest.* **99**:2351–2357.
43. Carmeliet, P., et al. 1999. Impaired myocardial angiogenesis and ischemic cardiomyopathy in mice lacking the vascular endothelial growth factor isoforms $VEGF_{164}$ and $VEGF_{188}$. *Nat. Med.* **5**:495–502.
44. Gerber, H.-P., et al. 1999. VEGF is required for growth and survival in neonatal mice. *Development*. **126**:1149–1159.
45. Tufró, A. 2000. VEGF spatially directs angiogenesis during metanephric development *in vitro*. *Dev. Biol.* **227**:558–566.
46. Roberts, W.G., and Palade, G.E. 1995. Increased microvascular permeability and endothelial fenestration induced by vascular endothelial growth factor. *J. Cell Sci.* **108**:2369–2379.
47. Esser, S., et al. 1998. Vascular endothelial growth factor induces endothelial fenestrations in vitro. *J. Cell Biol.* **140**:947–959.
48. Carmeliet, P., et al. 1996. Abnormal blood vessel development and lethality in embryos lacking a single VEGF allele. *Nature*. **380**:435–439.
49. Ferrara, N., et al. 1996. Heterozygous embryonic lethality induced by targeted inactivation of the VEGF gene. *Nature*. **380**:439–442.
50. McCright, B., et al. 2001. Defects in development of the kidney, heart and eye vasculature in mice homozygous for a hypomorphic *Notch2* mutation. *Development*. **128**:491–502.
51. Quaggin, S.E., et al. 1999. The basic-helix-loop-helix protein Pod1 is critically important for kidney and lung organogenesis. *Development*. **126**:5771–5783.
52. Noakes, P.G., et al. 1995. The renal glomerulus of mice lacking s-laminin/laminin β2: nephrosis despite molecular compensation by laminin β1. *Nat. Genet.* **10**:400–405.
53. Putaala, H., Soininen, R., Kilpeläinen, P., Wartiovaara, J., and Tryggvason, K. 2001. The murine nephrin gene is specifically expressed in kidney, brain and pancreas: inactivation of the gene leads to massive proteinuria and neonatal death. *Hum. Mol. Genet.* **10**:1–8.
54. Lehtonen, S., et al. 2000. *In vivo* interaction of the adapter protein CD2-associated protein with the type 2 polycystic kidney disease protein, polycystin-2. *J. Biol. Chem.* **275**:32888–32893.
55. Brogan, M., Chabanis, S., Schwarz, K., Shankland, S.J., and Mundel, P. 1991. Synaptopodin limits podocyte damage in experimental glomerulonephritis. *J. Am. Soc. Nephrol.* **12**:672a. (Abstr.)
56. Barbaux, S., et al. 1997. Donor splice-site mutations in *WT1* are responsible for Frasier syndrome. *Nat. Genet.* **17**:467–470.
57. Patek, C.E., et al. 1999. A zinc finger truncation of murine WT1 results in the characteristic urogenital abnormalities of Denys-Drash syndrome. *Proc. Natl. Acad. Sci. USA*. **96**:2931–2936.
58. Pelletier, J., et al. 1991. Germline mutations in the Wilms' tumor suppressor gene are associated with abnormal urogenital development in Denys-Drash syndrome. *Cell*. **67**:437–447.
59. Iida, K., et al. 1997. Essential roles of the winged helix transcription factor MFH-1 in aortic arch patterning and skeletogenesis. *Development*. **124**:4627–4638.
60. Kume, T., Deng, K., and Hogan, B.L.M. 2000. Murine forkhead/winged helix genes *Foxc1* (*Mf1*) and *Foxc2* (*Mfh1*) are required for the early organogenesis of the kidney and urinary tract. *Development*. **127**:1387–1395.
61. Kidson, S.H., Kume, T., Deng, K., Winfrey, V., and Hogan, B.L.M. 1999. The forkhead/winged-helix gene, *Mf1*, is necessary for the normal development of the cornea and formation of the anterior chamber in the mouse eye. *Dev. Biol.* **211**:306–322.
62. Dreyer, S.D., et al. 2000. *LMX1B* transactivation and expression in nail-patella syndrome. *Hum. Mol. Genet.* **9**:1067–1074.
63. Lennon, G., Auffray, C., Polymeropoulos, M., and Soares, M.B. 1996. The I.M.A.G.E. Consortium: an integrated molecular analysis of genomes and their expression. *Genomics*. **33**:151–152.